LETTER

Transcriptional activation of polycomb–repressed genes by ZRF1

Holger Richly[1], Luciana Rocha-Viegas[1], Joana Domingues Ribeiro[1], Santiago Demajo[1], Gunes Gundem[2], Nuria Lopez-Bigas[2], Tekeya Nakagawa[3], Sabine Rospert[4], Takashi Ito[3] & Luciano Di Croce[1,5]

Covalent modification of histones is fundamental in orchestrating chromatin dynamics and transcription[1–3]. One example of such an epigenetic mark is the mono-ubiquitination of histones, which mainly occurs at histone H2A and H2B[4–6]. Ubiquitination of histone H2A has been implicated in polycomb-mediated transcriptional silencing[7–9]. However, the precise role of the ubiquitin mark during silencing is still elusive. Here we show in human cell lines that ZRF1 (zuotin-related factor 1) is specifically recruited to histone H2A when it is ubiquitinated at Lys 119 by means of a novel ubiquitin-interacting domain that is located in the evolutionarily conserved zuotin domain. At the onset of differentiation, ZRF1 specifically displaces polycomb-repressive complex 1 (PRC1) from chromatin and facilitates transcriptional activation. A genome-wide mapping of ZRF1, RING1B and H2A-ubiquitin targets revealed its involvement in the regulation of a large set of polycomb target genes, emphasizing the key role ZRF1 has in cell fate decisions. We provide here a model of the molecular mechanism of switching polycomb-repressed genes to an active state.

To identify proteins capable of binding ubiquitinated H2A (H2Aub), we developed an affinity purification based on the expression of Flag-tagged histone H2A. Among several potential H2Aub-binding proteins (Supplementary Fig. 1A, C and Supplementary Table 1), we chose to analyse ZRF1 in more depth, as within its carboxy terminus this protein contains two SANT domains, which are often found in subunits of chromatin-remodelling complexes (Fig. 1a). Intriguingly, its yeast homologue Zuo1 is linked to the ubiquitination of histone H2B in *Saccharomyces cerevisae*[10]. Moreover, ZRF1 has also been implicated in cancer and differentiation[11–13]. It adopts an oligomeric conformation and is located in the nucleus as well as in the cytosol (Supplementary Figs 1D, E and 2A). Purification of mononucleosomes from 293T cells expressing Flag-tagged histone H2A, either wild type or mutated (KKRR) at the ubiquitination sites (K118/K119), revealed ubiquitin-specific ZRF1 binding preferentially to the wild-type mononucleosomes (Fig. 1b and Supplementary Fig. 1B, F, H, I). Corroborating this finding, we observed specific binding of ubiquitinated wild-type nucleosomes to recombinant ZRF1 (Fig. 1c). Thus, these data point to the ubiquitin mark at histone H2A as a docking site for ZRF1.

ZRF1 shares homology in the zuotin domain with its yeast orthologue Zuo1 (Fig. 1a), which is synthetically lethal with Rad6, the E2 enzyme involved in the specific ubiquitination of histone H2B[10]. We reasoned that the conserved zuotin domain might contain the ubiquitin-binding motif[14]. Results from pull-down experiments with a GST–ubiquitin fusion protein and different recombinant ZRF1 truncation proteins allowed us to map the ubiquitin-binding domain (UBD) to a region C-terminal of the DnaJ domain (Fig. 1d). H2A ubiquitination as well as histone H3K27me3 are marks typically located in promoter regions of polycomb-silenced genes[15,16]. To test for ubiquitin-dependent recruitment of ZRF1 to chromatin, we established NT2 knockdown cell lines for ZRF1 or RING1B (a PRC1 subunit that is an E3 ligase; Fig. 1e). We

then analysed occupancy at several promoter regions of polycomb-repressed genes, including *PER1*, *NF1C* (Fig. 1f) and the well-characterized *HOX* genes[15,16]. ZRF1 enrichment at the promoters clearly depended on the abundance of RING1B and on H2Aub levels (Fig. 1g, h and Supplementary Fig. 1G).

It has been shown that PRC1 is tethered to chromatin by the interaction of its subunit PC1 with a trimethyl mark on Lys 27 of histone H3 (H3K27me3)[8,16]. Using purified mononucleosomes containing either wild-type H2A or the H2A(KKRR) mutant, we observed that co-purification of the PRC1 subunits RING1B and BMI1 depended on the ubiquitination of histone H2A (Fig. 2a). In contrast, we did not find an alteration of the H3K27 methylation levels in nucleosomes devoid of the ubiquitin mark, indicating that stable maintenance of PRC1 at chromatin depends on the ubiquitin mark (Fig. 2a and Supplementary Fig. 2J). To understand the functional relationship between ZRF1 and PRC1, we characterized further the binding affinity of RING1B towards the ubiquitin residue by GST pull-down experiments (Supplementary Fig. 2B). Furthermore, after reconstituting RING1B-containing mononucleosome complexes, RING1B was efficiently released from nucleosomes following incubation with GST–ubiquitin (Fig. 2b and Supplementary Fig. 2C). This finding indicated that ZRF1 could compete with RING1B for binding at H2Aub. Indeed, ZRF1 overexpression led to displacement of the PRC1 subunits RING1B and BMI1 from chromatin, whereas ZRF1 knockdown led to an enhanced occupancy of RING1B at chromatin that caused an increase in H2A ubiquitination (Fig. 2c, d and Supplementary Fig. 2D–H). We next performed competition assays with the GST–ubiquitin substrate. When the His-tagged RING1B concentration was maintained, we observed that increasing the His–ZRF1 concentration led to a reduction of RING1B bound to the ubiquitin substrate, emphasizing the competition for the ubiquitin residue by both proteins (Fig. 2e). We then assembled recombinant RING1B–GST–ubiquitin complexes and performed pull-down experiments after adding either bovine serum albumin (BSA) alone (lane 1) or recombinant His–UBD and BSA (lanes 2 and 3). In concordance with the previous result, we observed RING1B replaced by the UBD of ZRF1 (Fig. 2f). Similarly, on reconstituted RING1B–mononucleosome complexes, ZRF1 efficiently displaced RING1B (Fig. 2g and Supplementary Fig. 2I). Finally, chromatin immunoprecipitation (ChIP) experiments in 293T cells overexpressing either ZRF1 or only the UBD, indicated an enrichment of ZRF1 or the UBD at promoters of the *HOX* gene cluster concomitantly with the displacement of the PRC1 subunits RING1B and BMI1 (Fig. 2h–i and Supplementary Fig. 2F). In contrast, neither a ZRF1 deletion mutant devoid of the UBD nor the yeast homologue Zuo1, which shows only a weak ubiquitin-binding capacity, were recruited to chromatin or were able to displace PRC1 (Supplementary Fig. 3A–C). It has been shown that depletion of RING1B, and thus H2A ubiquitination, leads to the loss of PRC2 from chromatin[17]. In agreement with this previous study, we found that PRC2 levels were reduced at KKRR mutant nucleosomes.

[1]Centre de Regulació Genòmica (CRG)/UPF, 08003 Barcelona, Spain. [2]Department of Experimental and Health Sciences, Universitat Pompeu Fabra, 08003 Barcelona, Spain. [3]Nagasaki University School of Medicine, Nagasaki 852-8523, Japan. [4]Institut für Biochemie und Molekularbiologie (ZBMZ), Universität Freiburg, 79104 Germany. [5]Institució Catalana de Recerca i Estudis Avançats (ICREA), Centre de Regulació Genòmica (CRG), PRBB, c/ Dr. Aiguader 88, 08003 Barcelona, Spain.

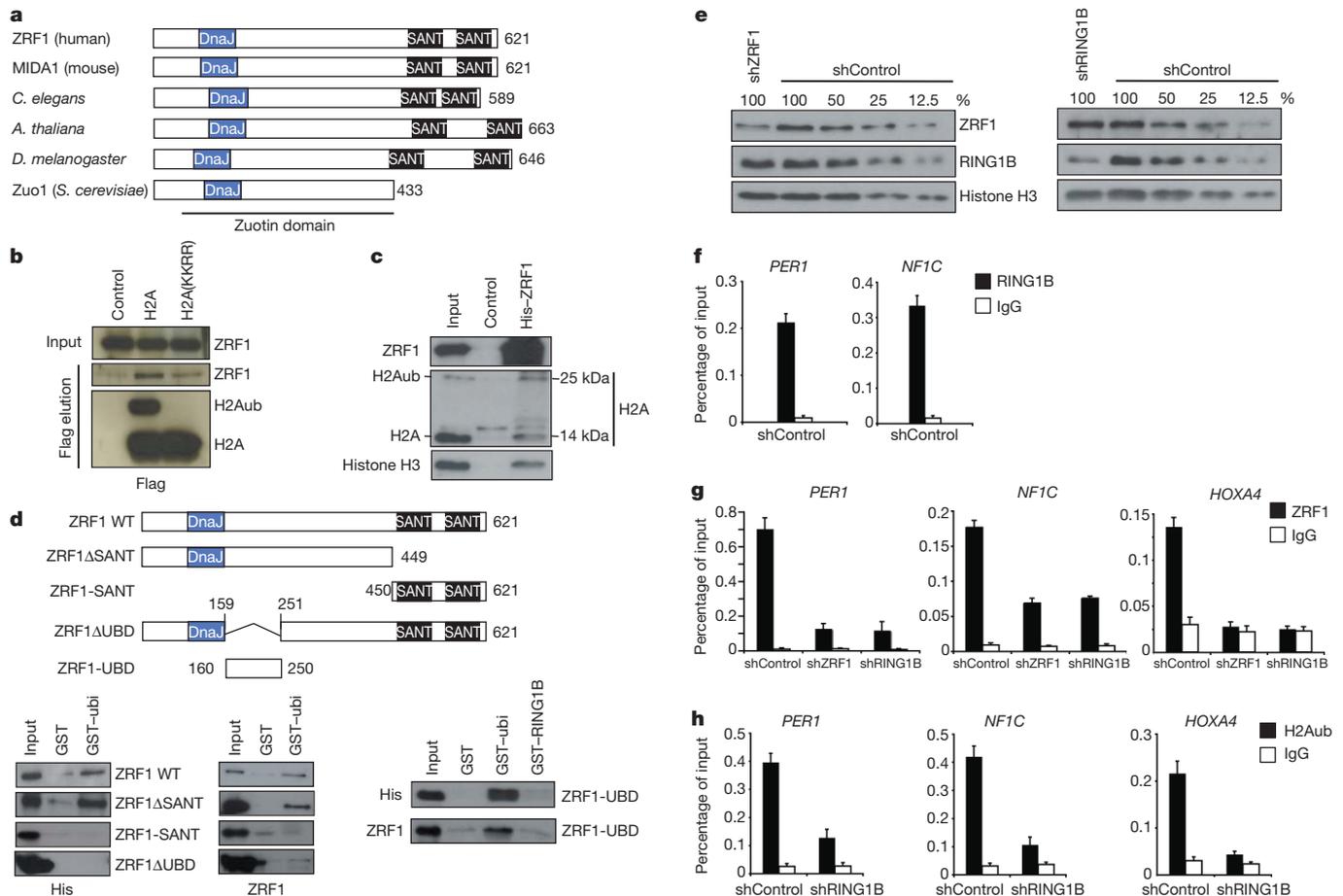**Figure 1 | ZRF1 interacts with H2Aub. a**, Schematic diagram of ZRF1 orthologues indicating the DnaJ domain and SANT domains. The numbers along the right-hand side of panels **a** and **d** refer to the number of amino acids each of the proteins is composed of. **b**, Flag-tagged histone H2A and H2A(KKRR) were expressed in 293T cells. Mononucleosomes were purified and eluates were subjected to immunoblot analysis using ZRF1 and Flag antibodies. The inputs correspond to 3%. **c**, Nuclear protein extracts containing mononucleosomes were incubated with recombinant His–ZRF1. Precipitated ZRF1–nucleosome complexes were subjected to immunoblot analysis using the indicated antibodies. The inputs represent 5% of His–ZRF1 and 2% of the protein extract. **d**, GST pull-downs with GST, GST–ubiquitin (GST–ubi) and GST–RING1B (right panel) and the His-tagged proteins indicated. Bound material was subjected to immunoblot analysis using His and ZRF1 antibodies. The input shown represents 2%. WT, wild type. **e**, Protein extracts of RING1B and ZRF1 knockdown cell lines were subjected to immunoblotting and probed with the antibodies indicated in the figure. **f**, ChIP experiments performed in NT2 control cells with RING1B antibodies. **g**, **h**, ChIP experiments performed in the NT2 control and knockdown cells with ZRF1 and H2Aub antibodies. The occupancy at promoters of the *PER1*, *NF1C* and *HOXA4* genes was tested by quantitative PCR. Data are represented as mean ± s.e.m. (*n* = 3).

Similarly, PRC2 levels decreased upon binding of ZRF1 to chromatin (Supplementary Fig. 4A–C).

To globally identify ZRF1 target genes, we performed a ChIP-on-chip (see Methods) analysis in NT2 cells[18,19]. Because our data indicate that ZRF1 might antagonize silencing by polycomb proteins, we designed an experiment that allowed us to study the occupancy of ZRF1 under conditions of retinoic-acid-induced differentiation (Fig. 3a). We found ZRF1 to be enriched in 758 (not induced), 2,295 (induced for 1 h) or 995 (induced for 3 h) genes (Fig. 3b and Supplementary Table 2). Analysis of the ZRF1 occupancy at its target genes revealed a marked increase at 1 h of induction (Fig. 3b, Supplementary Fig. 5C and Supplementary Table 2). Clustering the target genes with respect to their cellular functions indicates a role for ZRF1 in developmental processes and differentiation (Fig. 3c, d and Supplementary Fig. 5A, B). Additional ChIP-on-chip analysis indicates that RING1B and H2Aub target genes are mainly involved in developmental processes (Supplementary Figs 7A–L, 8A–J and Supplementary Tables 4 and 5), as shown in previous publications[20,21]. The overlap of ZRF1 targets (1 h retinoic acid) with RING1B and H2Aub targets led to the identification of 1,102 common target genes (Fig. 3e, f). Moreover, comparison of ZRF1 target genes with polycomb target genes[22] indicates that ZRF1 is more closely linked to PRC1 than to PRC2 (Supplementary Figs 6A, B, 8K, L). We next performed a gene expression analysis comparing short hairpin RNA targeting *ZRF1* (shZRF1) with shControl (non-specific shRNA constructs) cells, with or without retinoic-acid treatment. Interestingly, downregulated genes in shZRF1 after retinoic-acid stimulation are ZRF1 or polycomb targets, particularly for PRC1 and H2Aub (Supplementary Figs 6C, 9A–G and Supplementary Table 6). Among these genes more than a hundred are targeted by ZRF1, RING1B and H2Aub and many of these are major players in developmental pathways (Fig. 4a, b). To corroborate our findings, we performed ChIP experiments and gene expression analysis on selected ZRF1 target genes. We found that ZRF1 was significantly enriched at these genes only after stimulation with retinoic acid (Fig. 4c and Supplementary Fig. 10A). Under the same conditions, we observed transcriptional activation of the same genes in wild-type NT2 cells. However, in ZRF1 knockdown cells, we detected a decrease of the messenger RNA levels (Fig. 4d and Supplementary Fig. 10B). In sum, the data presented show a clear involvement of ZRF1 in the PRC1 pathway and, most importantly, that activation of genes targeted by PRC1 and H2Aub is facilitated by ZRF1.

Several polycomb target genes become activated during differentiation, concomitantly with the disappearance of the polycomb-dependent repressive marks[15,16,23,24]. Analysis of two *HOXA* genes revealed that retinoic-acid-induced transcriptional activation depended on the presence of ZRF1. In contrast, RING1B knockdown caused a more robust
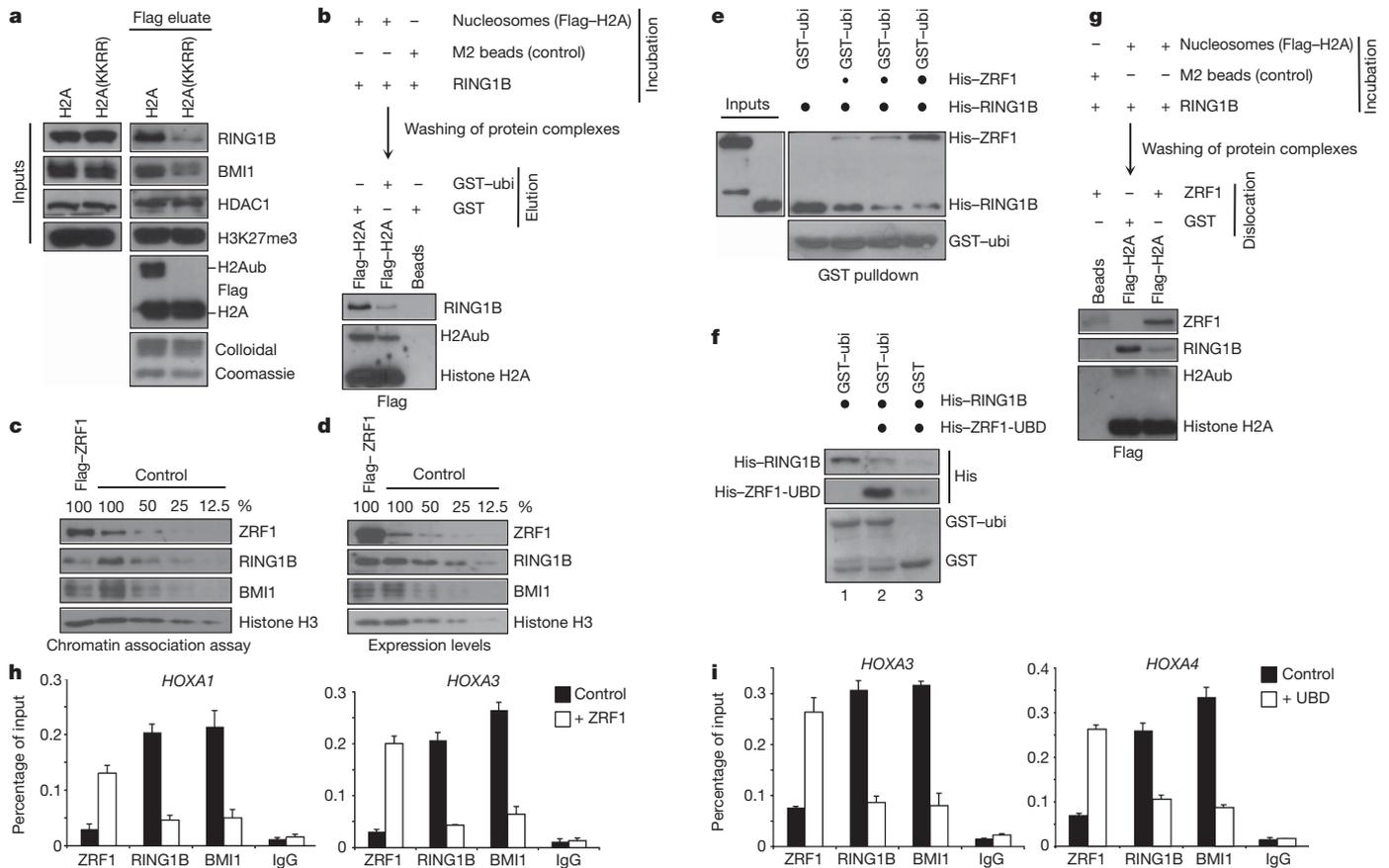
Figure 2 | ZRF1 and PRC1 compete for binding of H2Aub.
a, Mononucleosomes were purified from 293T cells expressing Flag-tagged H2A or a double mutant (KKRR). The purified material was subjected to immunoblot analysis using the indicated antibodies. The inputs represent 3%. **b**, Nucleosome–His–RING1B complexes were assembled, washed and incubated with GST (70 ng µl^{-1}) or GST–ubiquitin (70 ng µl^{-1}). Flag eluates were subjected to immunoblot analysis with the indicated antibodies. **c**, Chromatin association assay of 293T cells overexpressing ZRF1. Immunoblot analysis was performed with the indicated antibodies. **d**, Immunoblot analysis of 293T cells overexpressing ZRF1 using the indicated antibodies. **e**, GST–ubiquitin was incubated with constant amounts of His–RING1B and increasing amounts of His–ZRF1 finally reaching equimolar levels (last lane). The inputs show 10% of His–RING1B and 10% of the maximal amount of His–ZRF1.

f, GST and GST–ubiquitin were incubated with RING1B, washed and incubated with His–ZRF1-UBD (see Methods). The retained material was subjected to immunoblot analysis with His antibodies. Lane 1 shows the pull-down in the presence of only BSA, lanes 2 and 3 in the presence of both BSA and His–ZRF1-UBD. **g**, Nucleosome–His–RING1B complexes were assembled and incubated with GST (100 ng µl^{-1}) or ZRF1 (100 ng µl^{-1}). After elution by Flag peptide, immunoblot analysis was performed with Flag, RING1B and ZRF1 antibodies. **h**, ChIP experiments with ZRF1, RING1B and BMI1 antibodies after overexpression of ZRF1 in 293T cells. **i**, Experiments were performed as already stated with the exception that the Flag–UBD was overexpressed instead of the full-length ZRF1. The occupancy at promoters of *HOX* genes was tested with quantitative PCR. Data are represented as mean ± s.e.m. (n = 3).

activation of those genes, thus supporting opposing roles for PRC1 and ZRF1 in transcriptional regulation of promoters (Fig. 4e). Next we investigated the occupancy of both ZRF1 and RING1B at promoters of *HOX* genes during retinoic-acid-induced transcription. Retinoic-acid treatment led to the recruitment of ZRF1 to promoter regions with a concomitant reduction of RING1B occupancy, clearly indicating mutually exclusive binding for these proteins at chromatin (Fig. 4f, g). Accordingly, in ZRF1 knockdown cells, RING1B was not efficiently removed from chromatin after retinoic-acid induction (Fig. 4h), as supported by previous experiments (Fig. 2a–h). In related experiments (1 h retinoic acid) we found H2Aub to be slightly reduced at *HOXA* gene promoters, indicating a deletion of this histone mark shortly after the removal of PRC1 complexes (Supplementary Fig. 11A–C). A set of similar results was obtained in retinoic-acid-induced differentiation of leukaemic cells (Supplementary Fig. 10C–E)[24]. On the basis of our results, we reasoned that ZRF1 might facilitate transcription. Recently, it has been shown that USP21-mediated H2A deubiquitination precedes gene activation[25]. To investigate further the impact of ZRF1 on transcriptional activation, we performed *in vitro* experiments testing whether ZRF1 might act in concert with specific deubiquitinases. *In vitro* deubiquitination assays carried out with mouse liver chromatin demonstrate that ZRF1 facilitates H2A deubiquitination (Fig. 4i).

Thus, these results showed that, besides its function in the displacement of PRC1 complexes, ZRF1 facilitates transcription by cooperating with deubiquitinase enzymes.

Ubiquitination of H2A has long been correlated with activation of genes[26]. It is intriguing that ubiquitination of histone H2A not only has an effect on gene silencing but also is necessary to attract a factor that switches genes from a silenced to a transcriptionally activated state. However, it is still unclear how ZRF1 binding to chromatin is regulated (Supplementary Fig. 12A, B). One potential mode of regulating ZRF1, and thus cell differentiation, could be to mask its UBD domain. It has been shown that proteins of the ID (inhibitor of differentiation) family bind to ZRF1 in a region spanning its UBD domain[13] (Supplementary Fig. 12C). Our data indicate that association of PRC1 with chromatin depends on the H2Aub mark, whereas H3K27me3 is not sufficient to retain PRC1 complexes and is most probably required for its initial targeting[21,27]. RING1B/PRC1 are not as abundant as H2Aub, thus excluding a continuous binding of PRC1 complexes throughout chromatin. Yet it has been shown that during DNA damage H2A E3 ligases bind ubiquitinated H2A and propagate the initial chromatin ubiquitination marks[28]. A similar sliding mechanism could also apply to our findings regarding RING1B, and challenge the current view of ubiquitination and deubiquitination cycles (see also Supplementary
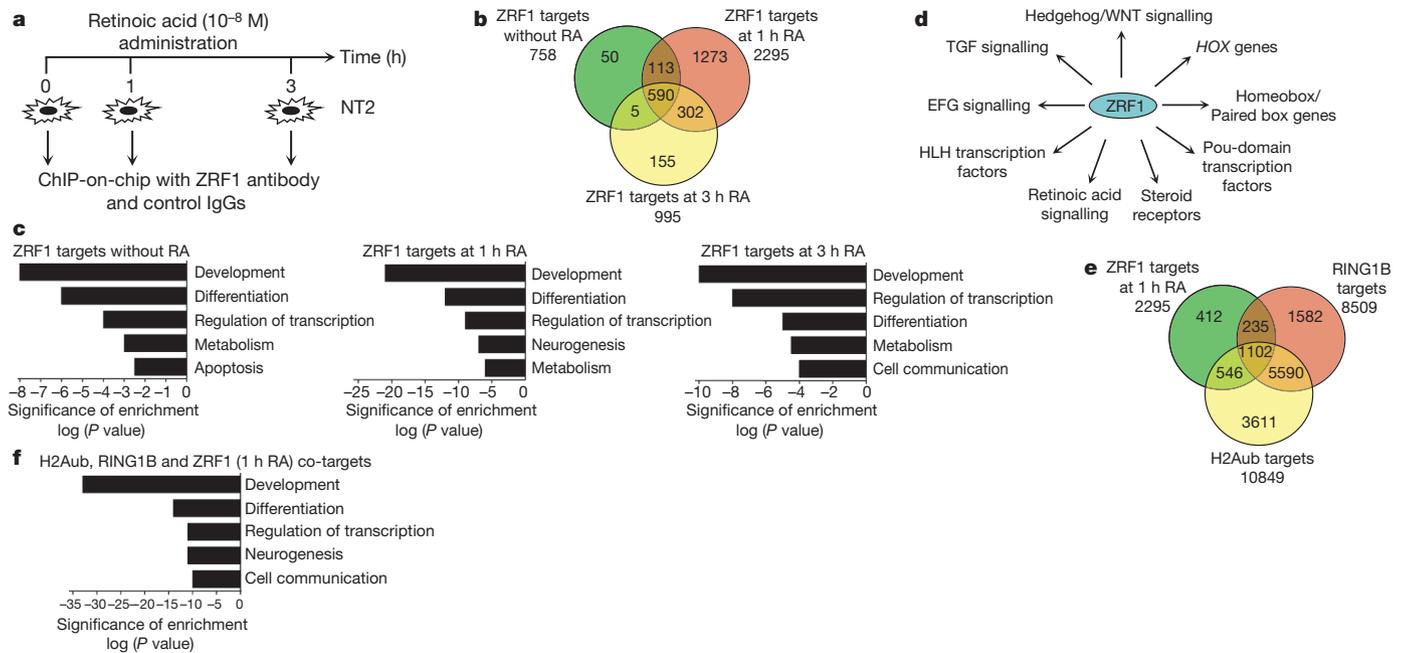
Figure 3 | Genome-wide mapping of ZRF1 target genes in NT2 cells.
a, Schematic representation of the experimental approach for the ChIP-on-chip experiment. Chromatin was subjected to triplicate ChIP experiments with ZRF1 and control antibodies. The obtained material was amplified and hybridized with Human Promoter Arrays chips from Agilent. **b**, Venn diagram of the ZRF1 target genes as obtained by Chipper analysis. **c**, Functional enrichment analysis of ZRF1 target genes at the different time points of retinoic-acid (RA) induction. **d**, A selection of ZRF1 target genes identified in this study (induced for 1 h), focusing on those known to be involved in key pathways controlling cell fate decisions. **e**, Venn diagram showing significant overlapping between the gene lists of RING1B, H2Aub and ZRF1 (induced for 1 h) as obtained by ChIP-on-chip analysis. The P values after overlapping the H2Aub target genes with ZRF1 and/or RING1B targets are listed in the following: RING1B ($P = 10^{-16}$), ZRF1 (1 h; $P = 10^{-12}$) and RING1B-ZRF1 co-targets ($P = 10^{-16}$). **f**, Functional enrichment analysis of the 1,102 common ZRF1/RING1B/H2Aub target genes.
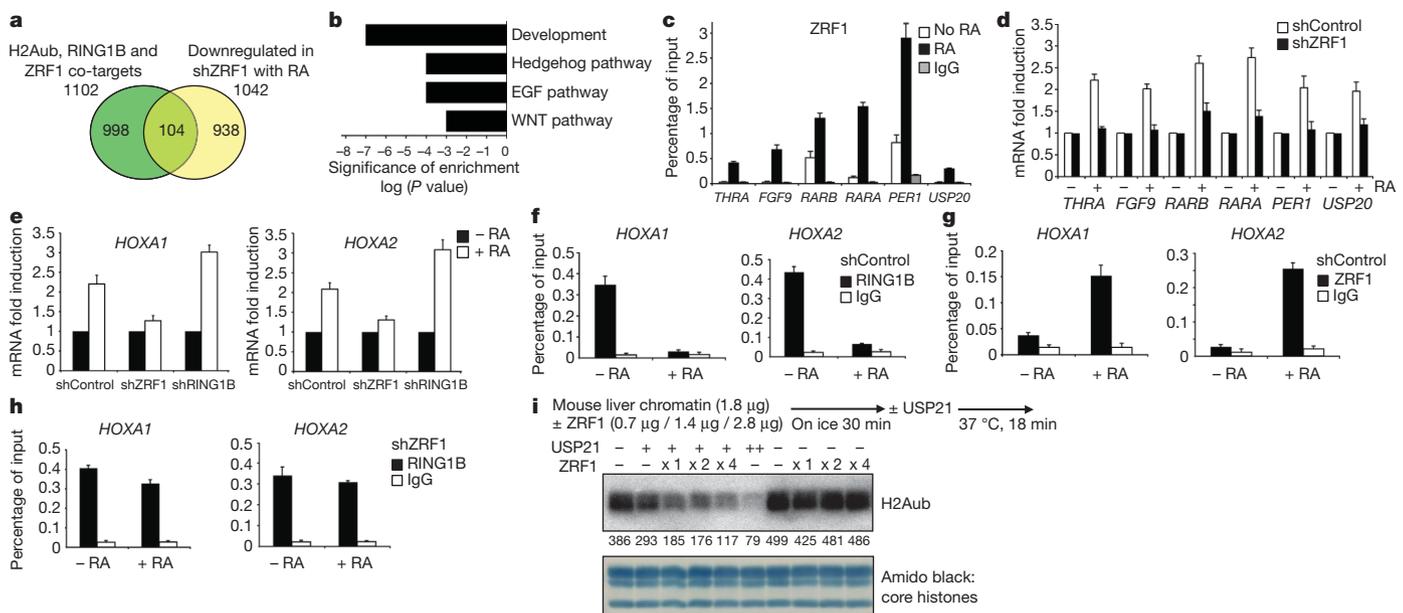

Figure 4 | ZRF1 functions in activating polycomb-repressed genes. a, The list of genes significantly repressed in comparison to shControl cells after stimulation with retinoic acid was overlapped with the common ZRF1/RING1B/H2Aub target genes (see also Supplementary Fig. 9). **b**, Functional enrichment analysis of the 104 common target genes downregulated in shZRF1 cells. **c**, ChIP experiments were performed with ZRF1 antibodies and chromatin obtained from NT2 induced with retinoic acid (THRA, FGF9, RARB and RARA: 1 h retinoic acid; PER1 and USP20: 3 h retinoic acid). The occupancy at promoters of the aforementioned genes was tested by quantitative PCR. Data are represented as mean ± s.e.m. ($n = 3$). **d**, The mRNA levels of the genes indicated were measured in NT2 shZRF1 and shControl cell lines after supplementing with retinoic acid for the respective times (THRA, FGF9, PER1 and USP20: 3 h retinoic acid; RARA and RARB: 2 h retinoic acid). Data are represented as mean ± s.e.m. ($n = 3$). **e**, shControl, shZRF1 and shRING1B NT2 cells were induced for 1 h with 10^{-8} M of retinoic acid. RNA levels of the HOXA1 and HOXA2 mRNA were measured in relation to mRNA levels of the ribosomal gene PUM1 ($n = 3$). **f–h**, shControl NT2 cells or shZRF1 knockdown cells were kept under the same conditions as in **e**, and chromatin was used in ChIP experiments with RING1B and ZRF1 antibodies. Data are represented as mean ± s.e.m. ($n = 3$). **i**, Mouse liver chromatin was incubated with ZRF1 and USP21 (10 or 20 ng) as indicated. The H2Aub levels were quantified after detection with specific antibodies.

Discussion). However, future research will have to reveal the dynamics of PRC1-catalysed ubiquitination.

METHODS SUMMARY

Experiments were performed using human cell lines (NT2, 293T and U937) and affinity-purified or commercially available antibodies. The knockdown cells used were established by retroviral infection. ChIP experiments, mutagenesis of histone H2A, genome-wide studies and protein purification procedures are explained in Methods.

Full Methods and any associated references are available in the online version of the paper at www.nature.com/nature.

1. Strahl, B. D. & Allis, C. D. The language of covalent histone modifications. *Nature* **403,** 41–45 (2000).
2. Li, B., Carey, M. & Workman, J. L. The role of chromatin during transcription. *Cell* **128,** 707–719 (2007).
3. Kouzarides, T. Chromatin modifications and their function. *Cell* **128,** 693–705 (2007).
4. Goldknopf, I. L. *et al.* Isolation and characterization of protein A24, a "histone-like" non-histone chromosomal protein. *J. Biol. Chem.* **250,** 7182–7187 (1975).
5. Zhu, B. *et al.* Monoubiquitination of human histone H2B: the factors involved and their roles in *HOX* gene regulation. *Mol. Cell* **20,** 601–611 (2005).
6. Nickel, B. E., Allis, C. D. & Davie, J. R. Ubiquitinated histone H2B is preferentially located in transcriptionally active chromatin. *Biochemistry* **28,** 958–963 (1989).
7. Wang, H. *et al.* Role of histone H2A ubiquitination in Polycomb silencing. *Nature* **431,** 873–878 (2004).
8. Kuzmichev, A., Nishioka, K., Erdjument-Bromage, H., Tempst, P. & Reinberg, D. Histone methyltransferase activity associated with a human multiprotein complex containing the Enhancer of Zeste protein. *Genes Dev.* **16,** 2893–2905 (2002).
9. Zhou, W. *et al.* Histone H2A monoubiquitination represses transcription by inhibiting RNA polymerase II transcriptional elongation. *Mol. Cell* **29,** 69–80 (2008).
10. Pan, X. *et al.* A DNA integrity network in the yeast *Saccharomyces cerevisiae. Cell* **124,** 1069–1081 (2006).
11. Greiner, J. *et al.* Characterization of several leukemia-associated antigens inducing humoral immune responses in acute and chronic myeloid leukemia. *Int. J. Cancer* **106,** 224–231 (2003).
12. Resto, V. A. *et al.* A putative oncogenic role for MPP11 in head and neck squamous cell cancer. *Cancer Res.* **60,** 5529–5535 (2000).
13. Inoue, T., Shoji, W. & Obinata, M. MIDA1, an Id-associating protein, has two distinct DNA binding activities that are converted by the association with Id1: a novel function of Id protein. *Biochem. Biophys. Res. Commun.* **266,** 147–151 (1999).
14. Hicke, L., Schubert, H. L. & Hill, C. P. Ubiquitin-binding domains. *Nature Rev. Mol. Cell Biol.* **6,** 610–621 (2005).
15. Bracken, A. P., Dietrich, N., Pasini, D., Hansen, K. H. & Helin, K. Genome-wide mapping of Polycomb target genes unravels their roles in cell fate transitions. *Genes Dev.* **20,** 1123–1136 (2006).
16. Lee, M. G. *et al.* Demethylation of H3K27 regulates polycomb recruitment and H2A ubiquitination. *Science* **318,** 447–450 (2007).
17. Saito, S. *et al.* Haptoglobin-β chain defined by monoclonal antibody RM2 as a novel serum marker for prostate cancer. *Int. J. Cancer* **123,** 633–640 (2008).
18. Andrews, P. W. Retinoic acid induces neuronal differentiation of a cloned human embryonal carcinoma cell line *in vitro. Dev. Biol.* **103,** 285–293 (1984).
19. Andrews, P. W. *et al.* Pluripotent embryonal carcinoma clones derived from the human teratocarcinoma cell line Tera-2. Differentiation *in vivo* and *in vitro. Lab. Invest.* **50,** 147–162 (1984).
20. Boyer, L. A. *et al.* Polycomb complexes repress developmental regulators in murine embryonic stem cells. *Nature* **441,** 349–353 (2006).
21. Kallin, E. M. *et al.* Genome-wide uH2A localization analysis highlights Bmi1-dependent deposition of the mark at repressed genes. *PLoS Genet.* **5,** e1000506 (2009).
22. O'Geen, H. *et al.* Genome-wide analysis of KAP1 binding suggests autoregulation of KRAB-ZNFs. *PLoS Genet.* **3,** e89 (2007).
23. Pasini, D., Bracken, A. P., Hansen, J. B., Capillo, M. & Helin, K. The polycomb group protein Suz12 is required for embryonic stem cell differentiation. *Mol. Cell. Biol.* **27,** 3769–3779 (2007).
24. Villa, R. *et al.* Role of the polycomb repressive complex 2 in acute promyelocytic leukemia. *Cancer Cell* **11,** 513–525 (2007).
25. Nakagawa, T. *et al.* Deubiquitylation of histone H2A activates transcriptional initiation via trans-histone cross-talk with H3K4 di- and trimethylation. *Genes Dev.* **22,** 37–49 (2008).
26. Levinger, L. & Varshavsky, A. Selective arrangement of ubiquitinated and D1 protein-containing nucleosomes within the *Drosophila* genome. *Cell* **28,** 375–385 (1982).
27. Lagarou, A. *et al.* dKDM2 couples histone H2A ubiquitylation to histone H3 demethylation during Polycomb group silencing. *Genes Dev.* **22,** 2799–2810 (2008).
28. Doil, C. *et al.* RNF168 binds and amplifies ubiquitin conjugates on damaged chromosomes to allow accumulation of repair proteins. *Cell* **136,** 435–446 (2009).

METHODS

Plasmids, antibodies and cell lines. Antibodies against ZRF1 and RING1B were either previously described[29], or raised in rabbits against full-length protein and affinity purified. To that end, GST fusion proteins of both proteins were cross-linked to glutathione beads and packed into polystyrol mini-columns (Pierce). Antisera were repeatedly run over the columns, washed and finally eluted in Tris buffer pH 2.5. The affinity-purified antibody was finally set to pH 8.0. For Fig. 1d the ZRF1 serum against full-length protein was used to visualize the recombinant protein deletion mutants. In all other experiments the antibody purified with GST–ZRF1ΔSANT (a ZRF1 protein lacking the C-terminal SANT domains) was used. Antibodies against H2Aub, IgM conjugating antibody and H3K4 trimethyl were obtained from Upstate antibodies. Antibodies against histone H2A and the histone modification H3K4 trimethyl were purchased from Abcam. Antibodies against the His and Flag epitopes were purchased from Qiagen and SIGMA, respectively. Antibodies against EED and SUZ12 were a gift from K. Helin. Plasmids for the ectopic expression of Flag-tagged ID proteins were a gift from J. Hasskarl. For tagging proteins the pet28 (His tag, Novagen), pCMV2 (Flag, Invitrogen) and pGex (GST, Invitrogen) vector series were used. The ZRF1 specific sequences GTTATCTGATCCAGTGAAA and GATCAAAGCAGCTCATAAA were used to synthesize oligonucleotides and cloned into the pRetroSuper[30]. In the case of RING1B the specific sequences AGAACACCATGACTACAAA and TTCTAAAGCTAACCTCACA were cloned into the same vector. Mutagenesis of histone H2A was performed using the Quikchange mutagenesis kit (Stratagene) on a pCMV2b histone H2A plasmid. Information on the cloning and sequences are available upon request. The embryonic carcinoma cell line NTERA2 (NT2/D1) and HEK 293T cells were cultured in DMEM medium supplemented with 10% fetal bovine serum at 37 °C and 5% CO₂. NT2 cells were treated with retinoic acid to induce differentiation at the given concentrations for the mentioned time intervals. U937 cells were cultured in RPMI medium at 37 °C and 5% CO₂.

Purification of recombinant proteins. Proteins were purified as suggested by Qiagen (His-tagged proteins) and Amersham (GST-tagged proteins) after inducing BL21 bacterial strains transformed with the respective plasmids at an optical density of 0.5 with 0.2 mM of isopropyl-β-D-thiogalactoside either for 4 h at 37 °C or at 20 °C for 14 h.

Purification of ubiquitin-binding proteins. HEK 293T cells were transfected with pCMV2b-histone H2A or the corresponding empty vector (Control) and after 48 h mononucleosomes were purified by means of the Flag epitope as stated in Supplementary Fig. 1A, C. After harvesting by centrifugation, cells were resuspended in buffer A (10 mM HEPES pH 7.9, 1.5 mM MgCl₂, 10 mM KCl and 0.5 mM dithiothreitol (DTT), phenylmethylsulphonyl fluoride (PMSF)) and homogenized by 10 strokes in a Dounce homogenizer with a B-type pestle. After centrifugation, nuclei were resuspended in lysis buffer (137 mM NaCl, 2.7 mM KCl, 10 mM NaH₂PO₄, 2 mM KH₂PO₄, 0.1% Triton X-100, 0.5 mM DTT, PMSF) and sonified using a Diagenode Bioruptor to obtain mononucleosomes (4 °C, 4 cycles of 15 min, 'H' setting). Protein extracts were then subjected to centrifugation (16,100g, 4 °C, 30 min) to remove debris and incubated with M2-Flag Agarose beads. The bound material or the control beads (M2-beads incubated with protein extracts from control transfections) were poured in polystyrol mini-columns (Flag–H2A column and Control column), washed intensively with lysis buffer and then used subsequently in an affinity purification. To this end, a nuclear protein extract devoid of histone proteins was prepared from 293T cells as previously described[31]. In brief, nuclei were extracted by resuspension of cells in buffer A (10 mM HEPES pH 7.9, 1.5 mM MgCl₂, 10 mM KCl and 0.5 mM DTT, PMSF) and homogenized by 10 strokes in a Dounce homogenizer with a B-type pestle. The crude nuclei were resuspended in buffer C (20 mM HEPES pH 7.9, 25% (v/v) glycerol, 1.5 mM MgCl₂, 420 mM NaCl, 0.2 mM EDTA, 0.5 mM DTT and PMSF) and homogenized in a Dounce homogenizer (10 strokes, B-type pestle). The resulting protein suspension was stirred by a magnetic stirring bar for 30 min at 4 °C and then centrifuged at 25,000g in an SS34 rotor for 3 h. The resulting supernatant was dialysed against lysis buffer, and run in a loop over two polystyrol mini-columns (Flag–H2A column and Control column; see above). After intensive washing with lysis buffer the columns were incubated with a solution of lysis buffer with recombinant His-tagged ubiquitin previously purified by Ni-NTA Agarose (Qiagen) and gel filtration on a Superose 12 column. After eluting the ubiquitin-binding proteins, the columns were washed again in lysis buffer and mononucleosomes were subsequently eluted by a solution of Flag peptide in lysis buffer. Both eluates were subjected to electrophoresis, stained with colloidal coomassie, and possible interactors were subjected to MALDI-Fingerprint analysis.

Transfection and retroviral infection. Transfection of HEK 293T cells was usually performed by the calcium phosphate co-precipitation method as described[24]. pRS-based retrovirus was produced by transfecting the GP2-293 packaging cell line (Clontech). The collected retrovirus was subsequently used to transduce NT2 or

293T cell lines by spinoculation at 900g for 90 min at 32 °C in the presence of protamine sulphate. After incubating overnight at 37 °C the protocol was repeated for two consecutive days.

M2-Flag affinity chromatography. Purification of Flag-tagged proteins from 293T cells was essentially done as described earlier. All experiments with Flag-tagged histone H2A were performed in polystyrene mini-columns (Pierce) with subsequent elution using the Flag peptide (Sigma) at a concentration of 100 μg ml⁻¹ in PBS.

ZRF1–H2Aub interaction experiments. Nuclear protein extracts were prepared as described earlier to obtain mononucleosomes. The protein extract was then incubated with or without recombinant His–ZRF1 (lanes ZRF1 and Control in Fig. 1c) for 4 h at 4 °C. Ni-NTA Agarose was added and after 2 h of incubation at 4 °C the beads were washed intensively with lysis buffer. The precipitated material was then subjected to western blotting.

Nucleosome–RING1B complexes and *in vitro* assays. Mononucleosomes were purified as described earlier, but washed with lysis buffer containing 450 mM NaCL and maintained at the Flag-M2 Agarose beads. The bound nucleosomes and empty M2 beads were subsequently incubated with bacterial extracts in lysis buffer containing recombinant His–RING1B. After 2 h of incubation at 4 °C the beads were washed in the same buffer intensively (see Supplementary Fig. 2C). The RING1B–nucleosome complexes were then incubated with equal or equimolar amounts of either GST or GST–ubiquitin (Fig. 2b) or ZRF1 (Fig. 2g) in lysis buffer. After 2 h of incubation at 4 °C the beads were packed into polystyrole columns, washed and eluted with Flag peptide at 100 μg ml⁻¹. The eluate was finally subjected to immunoblotting.

ChIP. ChIP experiments were essentially performed as described[24]. For all experiments affinity-purified antibodies were used as described earlier. The immuno-precipitated DNA was quantified by real-time quantitative PCR (Roche Lightcycler). The primers for verifying the occupancy of the immunoprecipitated protein at chromatin are available upon request.

Genome-wide mapping of ZRF1 target genes (ChIP-on-chip). Chromatin from NT2 cells before (0 h) and after induction with retinoic acid (10⁻⁸ M) for 1 h or 3 h was subjected to ChIP experiments with ZRF1 and control antibodies. For each time-point of the ChIP experiments triplicates were carried out. The obtained material was amplified with the WGA kit (Sigma) and linear amplification of the material was tested in qPCR reactions with known ZRF1 targets. Labelling and hybridization to Agilent Human Promoter Arrays were carried out following the supplier's instructions. Analogously, chromatin from unstimulated NT2 cells was subjected to ChIP experiments with RING1B, H2Aub and the respective conjugating antibody. The obtained material was processed as described earlier.

Microarray analysis. Microarray analysis was performed after extracting a triplicate of three different biological samples of RNA from NT2 cells lines (shZRF1 and shControl) either from non-induced cells or cells induced with retinoic acid (10⁻⁸ M, 3 h). RNA was amplified, labelled and subsequently hybridized to a Human Genome Oligo Microarray (Agilent). Raw data were analysed using the Limma package.

Data analysis and statistics. Absolute foreground and background readings from channels were used as input to the chipper program. Default parameters were used as defined previously[32]. Chipper calculates q values (corrected P values), thus accounting for multiple testing corrections per probe. Probes with q values <0.05 were accepted as significant. Probes, which are significantly bound by ZRF1, were compared to those significantly bound by IgG to subtract IgG targets. ZRF1 targets were mapped to genes according to the information provided by Agilent. To study significant overlapping between genes bound by ZRF1 and genes bound by SUZ12, RING1B, H2Aub or the H3K27me3 mark, respectively, the enrichment analysis (EA) method was applied. The statistical significance (P value) was calculated using the binomial distribution. Significance levels were corrected for multiple comparisons with the Benjamini and Hochbert method. Functional enrichment analysis was performed with the DAVID software[33].

RNA preparation and analysis by quantitative PCR. RNA was extracted with the RNeasy mini kit (Qiagen) and transcribed to cDNA by reverse transcription using the AMV kit (Roche). The expression of the respective genes was assayed by quantitative real-time PCR (Roche Lightcycler). As a reference, the expression of GAPDH or PUM1 was measured for each experiment. The sequences of the primers are available upon request.

GST pull-down. Purified GST–proteins were bound in equimolar amounts to glutathione beads (Amersham) in binding buffer (20 mM Tris pH 8.0, 150 mM NaCl, 0.5% NP-40). Loaded beads were washed in the same buffer and used for incubation with recombinant proteins for 2 h at 4 °C. For the competition assay (Fig. 2e) with recombinant ZRF1 and RING1B, the amounts of RING1B were kept constant and the amounts of ZRF1 were increased with every consecutive pull-down until finally reaching equimolar conditions. For preassembling RING1B–ubiquitin complexes (Fig. 2f), GST and GST–ubiquitin were bound to beads,

washed and incubated with RING1B at 4 °C for 2 h. Loaded beads were then incubated with a roughly tenfold higher amount of ZRF1-UBD together with an excess of BSA—where stated—for 90 min at 4 °C. Finally, beads were washed intensively in binding buffer, denatured in SDS buffer, and subjected to electrophoresis and subsequent western blotting analysis.

Gel-filtration analysis. Gel-filtration was performed on an AEKTA-Explorer system (Amersham) using Superose12 or Superose6 columns (Amersham). After calibrating the column with specific proteins, a solution of recombinant protein in PBS was injected and the UV-elution profile was detected. To verify each volume of elution the fractions were subjected to western blotting by probing with specific antibodies.

Chromatin association assays. Cells were crosslinked with a solution of 1% formaldehyde in PBS for 10 min at 24 °C. Nuclei were prepared by resuspending the cell pellets in buffer A (100 mM Tris pH 7.5, 5 mM MgCl$_2$, 60 mM KCl, 0.5 mM DTT, 125 mM NaCl, 300 mM sucrose, 1% NP-40). After lysis on ice the nuclei were pelleted and resuspended in buffer B (100 mM Tris pH 7.5, 1 mM CaCl$_2$, 60 mM KCl, 0.5 mM DTT, 125 mM NaCl, 300 mM sucrose) and supplemented with 10 U of MNase I for 20 min at 37 °C. The reaction was stopped by adding EDTA. The chromatin was pelleted and resuspended in buffer C (1% SDS, 10 mM EDTA, 50 mM Tris pH 8.0) overnight at 4 °C. After centrifugation (16,100g, 2 min) the supernatant was used for western blotting.

***In vitro* deubiquitination assays.** Deubiquitination experiments were essentially performed as previously described[25]. In short, mouse liver chromatin was incubated with no or increasing amounts of recombinant ZRF1. Subsequently USP21 was added and reactions were incubated at 37 °C for 18 min.

29. Otto, H. *et al.* The chaperones MPP11 and Hsp70L1 form the mammalian ribosome-associated complex. *Proc. Natl Acad. Sci. USA* **102,** 10064–10069 (2005).
30. Brummelkamp, T. R., Nijman, S. M., Dirac, A. M. & Bernards, R. Loss of the cylindromatosis tumour suppressor inhibits apoptosis by activating NF-κB. *Nature* **424,** 797–801 (2003).
31. Dignani, J. D., Lebovitz, R. M. & Roeder, R. G. Accurate transcription initiation by RNA polymerase II in a soluble extract from isolated mammalian nuclei. *Nucleic Acids Res.* **11,** 1475–1489 (1983).
32. Gibbons, F. D., Proft, M., Struhl, K. & Roth, F. P. Chipper: discovering transcription-factor targets from chromatin immunoprecipitation microarrays using variance stabilization. *Genome Biol.* **6,** R96 (2005).
33. Huang, D. W., Sherman, B. T. & Lempicki, R. A. Systematic and integrative analysis of large gene lists using DAVID bioinformatics resources. *Nature Protocols* **4,** 44–57 (2009).